BIOCHEMISTRY
including biophysical chemistry & molecular biology
Article

Biochemistry **2010,** *49,* 4679–4686 4679
DOI: 10.1021/bi1003266

Structural Basis for the Non-Immunosuppressive Character of the Cyclosporin A Analogue Debio 025†

Isabelle Landrieu,[‡,#] Xavier Hanoulle,[‡,#] Fanny Bonachera,[‡] Arnaud Hamel,[§] Nathalie Sibille,[‡] Yanxia Yin,[⊥] Jean-Michel Wieruszeski,[‡] Dragos Horvath,[∥] Qun Wei,[⊥] Grégoire Vuagniaux,[§] and Guy Lippens*[,‡]

[‡]*Structural and Functional Glycobiology Unit, UMR8576 CNRS-Université des Sciences et Technologies de Lille, Lille, France,* [§]*Debiopharm, Lausanne CP211, Switzerland,* [∥]*ULP, Laboratoire d'Infochimie, UMR 7177, Strasbourg, France, and* [⊥]*Department of Biochemistry and Molecular Biology, Beijing Normal University, Beijing 100875, China* [#]*These authors contributed equally to this work.*

Received March 4, 2010; Revised Manuscript Received April 27, 2010

ABSTRACT: Debio 025 is a cyclosporin A (CsA) analogue that interferes strongly with the hepatitis C viral life cycle. Compared to CsA, Debio 025 has an additional methyl group at position 3 of the cyclic undecapeptide and an *N*-ethylvaline instead of an *N*-methylleucine at position 4. Unlike CsA, Debio 025 lacks immunosuppressive activity in vitro and in vivo. We show here that, in vitro, the cyclophilin A (CypA)−Debio 025 complex cannot interact any longer with calcineurin (CaN), a determinant for the immunosuppressive activity of CsA. We further use NMR spectroscopy to investigate at the molecular level the interaction of Debio 025 with CypA and thereby understand the basis for this loss of CaN interaction. NMR data and molecular modeling indicate that Debio 025 optimally interacts with CypA, which underlies the anti-HCV properties of Debio 025. However, the interaction between CaN and the CypA−Debio 025 complex is impeded by sterical hindrance of the CaN with the side chain of its Val4 residue. This is in sharp contrast with the case for the CypA−CsA−CaN ternary complex, where the Leu4 side chain can enter a hydrophobic cavity at the CaN interface. The structure of the CypA−Debio 025 complex thus provides a rational explanation for the non-immunosuppressive character of Debio 025.

Cyclosporin A (CsA), an 11-amino acid cyclic peptide produced by the fungus *Tolypocladium inflatum Gams*, is clinically used as an immunosuppressor to prevent graft rejection in organ transplantation. Several classes of drug-targeted cyclophilin (Cyp) prolyl *cis*/*trans* isomerases (*1*, *2*) have been described, including the cytoplasmic and nuclear CypA and the secreted and intra-endoplasmic reticulum-located CypB (*3*, *4*). Cyclophilins catalyze in vitro the *cis*/*trans* conversion of the peptide bond N-terminal to the prolyl residue (*5*). CsA inhibits this activity through overlap of its binding site with the catalytic pocket. Immunosuppression, however, is not linked to this inhibitory function. Rather, the novel molecular surface resulting from the tight CypA−CsA interaction allows the complex to inhibit the calmodulin-dependent (calcium-activated) protein phosphatase calcineurin (CaN) required for T-cell activation (*6*, *7*). Neither Cyp nor CsA alone can inhibit this phosphatase or its downstream pathway.

Beyond immunosuppression, CsA also inhibits human immunodeficiency virus type 1 (HIV-1) replication in human cells by targeting the endogenous Cyp of the infected cell (*8*, *9*). At an early step in the viral life cycle, prior to reverse transcription, CypA indeed interacts with the HIV-1 CA domain of the Gag polyprotein, thereby enhancing the viral infectivity in humans (*8*, *10*). More recently, the CypA−CA interaction was shown to alter the recognition of the virus by host restriction factors (*11*, *12*). Drugs such as CsA that disrupt the CypA−Gag interaction can inhibit the replication of HIV-1 in tissue culture (*13*).

In addition, CsA inhibits the in vitro replication of hepatitis C virus (HCV) in HCV replicons (*14*) and human hepatocytes infected with HCV (*15*, *16*), with the endogenous Cyp as a molecular target (*17*). Conflicting results with respect to which Cyp is essential for HCV replication exist as CsA inhibits Cyp proteins in the nanomolar range (*18*). A decreased level of active CypB, but not CypA, was initially shown to inhibit the accumulation of HCV RNA in the HCV replicons (*19*). However, the essential role of CypA for HCV replication was subsequently demonstrated (*17*, *20*−*25*), and cyclosporine resistance development in vitro has also been linked to this cyclophilin (*20*, *21*).

Because the HCV replicons do not encode structural proteins of the virus (*14*), a parallel mechanism for Cyp in HIV and HCV infectivity can be eliminated. A direct binding of Cyp to the nonstructural protein 5B (NS5B) was proposed as the molecular mechanism underlying both CypB (*19*, *26*, *27*) and CypA (*20*, *23*) function. A direct interaction between CypA and NS5A (*28*) and the analysis of CsA resistance mutations (*21*, *24*, *27*, *29*) both indicate that NS5A, involved in a poorly understood manner in viral replication and particle production, may also be targeted by CypA. CypA could also functionally interact with additional viral proteins, presumably NS2, which is involved in polyprotein processing (*30*). The roles of CypA in HCV replication and virus production might thus be multiple and await further elucidation.

HCV causes serious liver diseases, treated currently with a combination of the antiviral ribavirin and pegylated interferon (*31*, *32*). This therapeutic protocol has proven to be effective only in a fraction of patients, hence the necessity of new treatments. Initiated

†The NMR facility was financed by the Conseil Régional Nord-Pas de Calais, the Pasteur Institute of Lille, the University of Lille 1, and the CNRS. Part of this study was sponsored by Debiopharm (Lausanne, Switzerland).

*To whom correspondence should be addressed. E-mail: Guy.lippens@univ-lille1.fr. Telephone: +33 3 20337241. Fax: +33 3 20436555.

Published on Web 04/28/2010

by the discovery of its antiviral activities, new drugs based on the CsA peptide structure have been under investigation (*33*−*36*). Debio 025 is such a CsA analogue, which differs from CsA with the replacement of the nonnatural amino acid sarcosine at position 3 with D-Ala and at position 4 with the replacement of *N*-methylleucine with *N*-ethylvaline (*37*).

A promising antiviral drug candidate, Debio 025 has superior antiviral activity compared to that of CsA in inhibition experiments based on HCV replicons (*38*, *39*). Debio 025 is indeed able to clear hepatocyte cells from their replicons, while CsA is unable to do so at comparable concentrations. Debio 025 is also tolerated better than CsA in virus-infected chimeric mice, with good antiviral activity in this in vivo model when used in combination with pegylated interferon (*40*). The Debio 025 anti-HCV effect has been confirmed in patient studies, alone in patients coinfected with HCV and HIV (*41*), or in combination with PEG interferon (*42*) and has now progressed to phase 2b studies.

Most importantly, Debio 025 was shown to have significantly decreased or no immunosuppressive activity compared to that of CsA, indicating that its antiviral activity is independent of its immunosuppressive activity. Debio 025 exhibited a much lower activity than CsA in an NFAT-dependent IL-2 reporter gene assay and in a murine mixed lymphocyte reaction (*43*). Unlike CsA, Debio 025 did not inhibit calcineurin-dependent translocation of GFP-NFAT to the nucleus in Jurkat T cells, nor does it prevent activation of resting mouse T lymphocytes (*44*). In the rat KLH model, treatment with Debio 025 at 10, 25, or 50 mg/kg for 4 weeks did not have an effect on the IgM response or influence the relative amounts of lymphocyte subpopulations, whereas 10 mg of CsA/kg significantly reduced anti-KLH IgM levels as well as T-lymphocyte and cytotoxic T-cell populations (*43*).

Whereas this suggests that the CypA−Debio 025 complex has less affinity for CaN than the CypA−CsA complex, formal proof of this has been lacking. Using size exclusion chromatography, we first investigate the formation of the ternary complex of the CypA−Debio 025 or CypA−CsA complex with CaN. Although CypA and Debio 025 form a complex with nanomolar affinity, the resulting binary complex is unable to assemble into a ternary complex with CaN, in agreement with its lack of immunosuppression activity. This is in stark contrast with the CypA−CsA complex that forms a stable ternary complex with CaN. Because understanding the non-immunosuppressive character of CsA analogues such as Debio 025 is a *conditio sine qua non* for their clinical use as antivirals and might eventually lead to the development of even better antivirals, we set out to study the structural aspects of Debio 025 when it interacts with human CypA. On the basis of experimental data for both the ligand and the protein in the complex and the existing crystallographic structure of the CypA−CsA complex (*45*), Debio 025 was found to occupy the active site of CypA in a manner closely resembling that of CsA. Molecular modeling starting with our NMR-derived CypA−Debio 025 structure and the X-ray structure of the CypA−CsA−CaN complex [Protein Data Bank (PDB) entry 1M63 (*46*)] allows us to explain at the molecular level the non-immunosuppressive character of the Debio 025 molecule. Whereas the CaN hydrophobic pocket is optimally occupied by the Leu4 side chain in the complex with the CypA−CsA binary complex, the Val4 side chain of Debio 025 cannot enter this pocket and thereby impedes the formation of a stable ternary complex. We thus conclude that the non-immunosuppressive character of Debio 025 stems from an impaired interaction of the CypA−Debio 025 complex with CaN because of the replacement of the *N*-methylleucine at position 4 of CsA with *N*-ethylvaline in Debio 025.

METHODS

Preparation of Isotope-Labeled Recombinant CypA Protein. The CypA cDNA was inserted in the pET15b vector that contained an efficient T7lac promoter driving the expression of CypA fused to an N-terminal His tag in *Escherichia coli* strain BL21(DE3)star. Induction was achieved via addition of 0.4 mM isopropyl β-D-thiogalactopyranoside (IPTG). For stable isotope labeling, the bacteria were grown in minimal medium (M9) with $^{15}NH_4Cl$ as the sole nitrogen source and/or [^{13}C]glucose as the carbon source. [^{15}N,^{2}H]CypA production was more difficult as bacteria had to be grown in deuterium and the glucose was also deuterated (glucose-d_7, Isotech). We used a modified version of M9 medium, supplemented with 10% rich labeled medium (Isogro, Isotech). To minimize the addition of water to the culture, the inoculum was directly collected from an agarose plate and diluted in the culture, yielding an A_{600} of 0.04. Bacteria were grown for ~24 h to reach a sufficient density before induction by IPTG. The culture was then pursued for 16 h at 20 °C before being harvested. Harvested bacteria were suspended in 50 mM NaP_i (pH 7.8) and 300 mM NaCl (buffer A) with 10 mM imidazole supplemented with protease inhibitors without EDTA (Roche) and 0.5% Triton X-100 and lysed via sonication after addition of lysozyme and DNase. The protein was then loaded on a nickel-NTA resin (HiTrap 1 or 5 mL column, GE Healthcare). Washing was conducted with buffer A with 50 mM imidazole and elution with a gradient from 50 to 250 mM imidazole. Concentrations of imidazole in extraction buffer and in washing buffer were optimized to yield a protein with good homogeneity in this single purification step (>95% pure). The protein was stored at 4 °C following buffer exchange against NMR buffer [50 mM NaP_i (pH 6.3), 20 mM NaCl, 1 mM DTT, and 2 mM EDTA] and concentrated using centrifugal concentrators (Vivaspin, cutoff of 10 kDa) to 8 mg/mL. CypA (20−40 mg) was obtained from 1 L of *E. coli* culture, depending of the labeling scheme, after purification from the bacterial extract.

NMR Samples of CypA Complexes. Debio 025 (D-MeAla3-*N*-EthVal4-cyclosporin) and CsA were obtained from DebioPharm S.A. Two analogues of CsA, chemically modified at the nitrogen of residue 4 with a methyl (MeVal4Cs) or an ethyl (EthVal4Cs) and without modification of residue 3, were kindly provided by Dr. Wenger (Wenger Chemtech, Riehen, Switzerland). To prepare CypA−ligand complexes, the ligand was directly added as powder to the protein solution because CsA and its analogues are poorly soluble in water. The mixture was kept at room temperature for 2 h on a rotating wheel before measurements were taken. The excess solid ligand was removed by centrifugation.

Size Exclusion Chromatography of CypA−CsA and CypA−Debio 025 Complexes and Calcineurin. Lyophilized calcineurin (subunits A and B) was dissolved in 50 mM Tris-HCl (pH 7.4), 100 mM NaCl, and 0.2 mM EDTA, and the remaining precipitate was removed by centrifugation. On the basis of UV measurements at 280 nm, the CaN protein concentration was estimated by UV (280 nm) to be 39 μM and the CypA, CypA−CsA, and CypA−Debio 025 samples were adjusted to 200 μM. CypA, CypA−CsA, and CypA−Debio 025 samples were mixed with calcineurin in a 1:5 ratio (6 μM to 29 μM) before being analyzed by size exclusion chromatography on a Superdex 200 HR10/30 column (GE Healthcare). Analysis of various fractions

by SDS−PAGE and Coomassie staining was performed after TCA precipitation of the proteins.

NMR Spectroscopy. All spectra were recorded on a Bruker Avance 800 MHz spectrometer with a standard triple-resonance probe head, at 293 K. The spectra were processed with Bruker TOPSPIN. The CypA−Debio 025 complex backbone assignment was performed by the classical strategy of three-dimensional (3D) triple-resonance NMR spectra on a 340 μM doubly labeled [^{15}N,^{13}C]CypA sample at 298 K. The chemical shifts of atoms of the free CypA backbone were obtained from K. Wutrich (Zurich, Switzerland) (*47*), and those of the CypA−CsA complex were retrieved from the BioMagResBank (entry 2208) (*48*). In both cases, chemical shift data were corrected for our experimental conditions through the recording and analysis of 3D HNCACB and HNCO experiments.

A two-dimensional (2D) NOESY spectrum (200 ms mixing time) was used to assign signals and to obtain conformational constraints of the bound Debio 025 in the [^{15}N,^{2}H]CypA−Debio 025 complex in D_2O phosphate buffer. The NOE-derived distances listed in Table S2 of the Supporting Information were obtained by normalization of the NOE peak integrals against integrals of intraresidual NOE peaks arising from identical chemical groups (for example, an ethyl group to a methyl group) separated by known distances. 2D natural abundance ^{1}H−^{13}C HMQC spectra of bound CsA and Debio 025 were recorded in D_2O phosphate buffer (*49*). On samples in aqueous buffer, we additionally recorded a 3D NOESY-HSQC spectrum of the [^{15}N,^{2}H]CypA−Debio 025 complex or CsA with a mixing time of 400 ms (*49*). The 2D ^{1}H−^{15}N HSQC spectra of the protein in the presence of ligands were recorded on [^{15}N]CypA in phosphate buffer to map the binding site of CsA, Debio 025, and additionally MeVal4Cs and EthVal4Cs.

Molecular Structures. To obtain starting coordinates of the Debio 025 ligand, CsA bound to CypA [PDB entry 1CWA (*45*)] was taken to be the template. Chemical groups of residues 3 and 4 in the peptide ring were manually modified using the Pymol builder (The PyMOL Molecular Graphics System, DeLano Scientific, San Carlos, CA). All nine possible rotamers were considered for residue 4 (three dihedral χ_1 angles, three dihedral CO_{i-1}−$N/_NC1$−$_NC2$ angles) before the energy minimization step performed with the DISCOVER module of Insight. After selection of the Debio 025 rotamer compatible with the observed NOEs, the structure of the complex was obtained via replacement of the CsA ligand in the CsA−CypA complex (PDB entry 1CWA) by superposition of the backbone of residues 7−10 of CsA with those of the minimized Debio 025. The experimental NMR data were then used to define the part of the molecules that were allowed to evolve during the energy minimization of the complex, residues 52−56, 63−76, and 101−112 for CypA and residues 6−11 for Debio 025. As a control for the procedure, the same protocol was followed to regenerate a minimized CsA−CypA complex. Further parameters for both minimizations (ligand alone and complex) were derived from the CVFF force field after charge assignment by ESFF. The dielectric constant was fixed at a value of 4.0, and 1000 conjugate gradient steps were performed. Pymol was used for graphical inspection of modeled proteins and ligands and to generate the various figures. A homology model of the CypA−Debio 025−CaN complex was obtained via replacement of the CypA−CsA complex in the 3D structure the CypA−CsA−CaN complex (*46*) with the CypA−Debio 025 complex structure obtained as described above, by superposition of the Cα atoms of residues 1, 2, and 8−11 of the ligands.

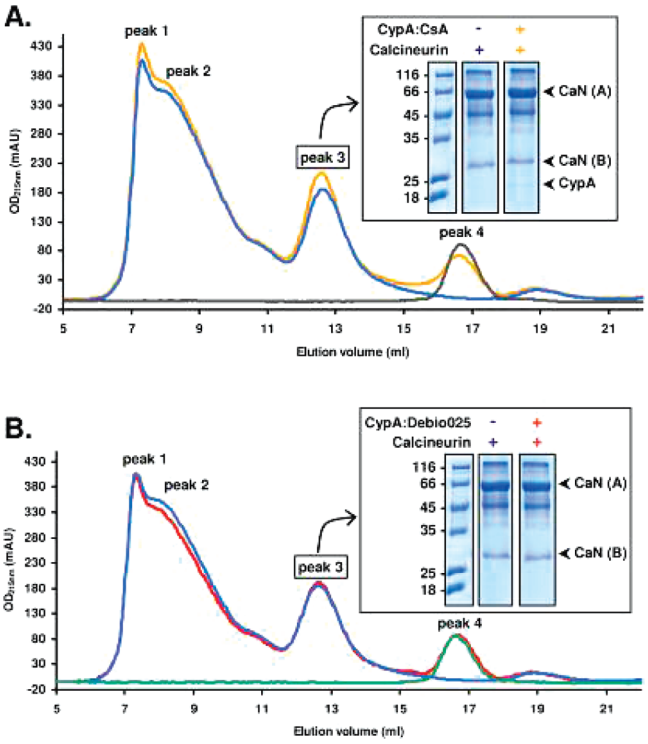

FIGURE 1: Superimposed chromatograms of the size exclusion analysis (Superdex 200) of (A) the CypA−CsA complex (black), CaN (blue), and the CypA−CsA complex with CaN (orange) and (B) the CypA-Debio 025 complex (green), CaN (blue), and the CypA−Debio 025 complex with CaN (red). Elution was monitored at 215 nm. The insets show the separation of the proteins collected as peak 3 (as annotated on the chromatogram) by SDS−PAGE followed by Coomassie blue staining.

RESULTS AND DISCUSSION

Interaction of CypA−CsA and CypA−Debio 025 Complexes with CaN. Debio 025 has lost its immunosuppressive character (*43*), resulting from the nonactivation of the NFAT pathway and thus most probably from a weakened interaction of the Debio025−CypA complex by CaN. To examine this hypothesis, the ability of CypA to interact with CaN (PP2B) was assessed in the presence of CsA or Debio 025 using size exclusion chromatography to detect formation of the ternary complex. Analysis of the isolated molecular components showed that CaN is partially present in a multimeric or aggregated form (peaks 1 and 2 in Figure 1), but the peak expected at the elution volume corresponding to CaN's molecular mass (~78 kDa) is well observed (peak 3 in Figure 1). When the CypA−CsA complex was mixed with CaN (Figure 1, orange curve), a shift and an increased intensity are observed for the monomeric CaN peak (peak 3; compare the blue and orange curves in Figure 1), while in parallel, the intensity of peak 4 corresponding to the binary CypA−CsA complex was reduced (peak 4; compare the black and orange curves in Figure 1). These changes indicate a molecular interaction between the CypA−CsA complex and CaN. To confirm the formation of the CypA−CsA−CaN ternary complex, samples of the various peaks were collected and analyzed by SDS−PAGE (13%). In the presence of CsA, peak 3 indeed contains CypA (inset in Figure 1A). Similar changes were not observed for the CypA−Debio 025 complex mixed with CaN. Both the elution peak of the CypA−Debio 025 complex and the peak corresponding to the monomeric fraction of CaN do not change when the three components are mixed together (in Figure 1, red

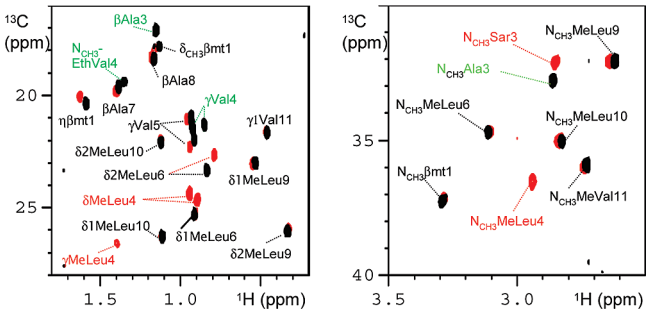

FIGURE 2: Annotated ^{1}H−^{13}C HMQC spectrum of the CypA-bound Debio 025 (black) and CsA (red) molecules recorded in natural abundance. The region showing the methyl resonances is annotated (except MeLeu11 Hγ at −0.69 ppm). Specific resonances of Debio 025 are annotated in green and those of CsA in red. Resonances corresponding to identical residues in both ligands are annotated in black.

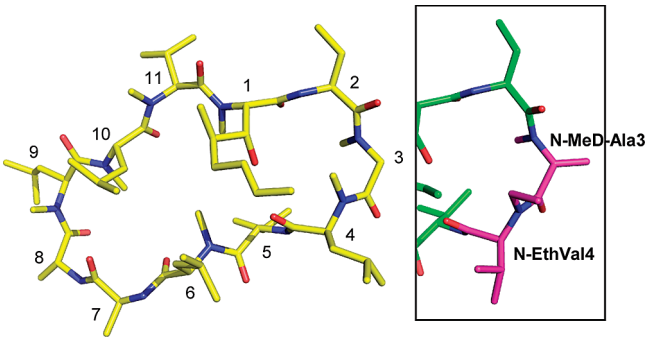

FIGURE 3: Model of the CsA (PDB entry 1CWA) molecule and comparison with the experimental model of the Debio 025 rotamer (boxed). Residues are represented as sticks, without hydrogen atoms, with nitrogens colored blue, oxygens red, and carbons yellow for CsA and green and pink for Debio 025. The chemical modifications in the Debio 025 molecules are highlighted in pink.

curve vs blue and green curves). Moreover, no CypA could be detected by SDS−PAGE in the CaN fraction (peak 3) of the ternary mixture fraction. Our observation that the CypA−Debio 025 complex does not form a ternary complex with CaN that can be isolated by size exclusion chromatography, provides a molecular basis for the non-immunosuppressive character of Debio 025.

Conformation of Debio 025 in the Complex with CypA. We next started a NMR study of the structure of Debio 025 in its complex with CypA, in an effort to understand the structural features that impair the interaction of the complex with CaN. The Debio 025 molecule differs from CsA in the presence of an additional methyl group on the Cα atom of the amino acid at position 3 (Sar3 to *N*-MeDAla3) and the replacement of *N*-MeLeu4 with *N*-EthVal4. Whereas earlier NMR studies used ^{13}C-labeled CsA isolated from the fermentation of the fungus in a ^{13}C-labeled medium (*49*, *50*), the chemical steps used to produce Debio 025 (*37*) made such an approach more problematic. A [^{15}N,^{2}H]CypA protein deuterated at all its positions (*51*) was used as an alternative to observe the ligand molecule without a protein background (*51*). Following this latter strategy, proton spectra of Debio 025 in its CypA-bound form were recorded without the interference of protein signals, and homonuclear NOESY and TOCSY experiments led to the full assignment of all Debio 025 resonances in the complex (Table S1 of the Supporting Information). We found excellent agreement with the published assignment of the CsA molecule bound to CypA (*48*, *50*). Comparison of the ^{1}H−^{13}C HMQC spectra of both ligands in their bound conformation confirms this conclusion and extends this near identity to the carbon chemical shifts (Figure 2). Only a few deviations of the chemical shifts are observed beyond the chemically modified residues, such as the Hδ2 methyl protons of the MeLeu6 residue or the Hη methyl protons of the Meβmt1[1] residue (Figure 2). The observed chemical shift conservation between Debio 025 and CsA in their complex with CypA is the first strong argument in favor of the conservation of the global conformation and binding mode for the two analogues.

The assignment of all the Debio 025 proton resonances was used to identify the conformation-dependent NOE cross-peaks in the [^{15}N,^{2}H]CypA−Debio 025 complex. Long-range cross-peaks were observed between the *N*-methyl protons of MeLeu6 and MeLeu11 of Debio 025, where both residues are located on opposite sides of the ring in CsA (Figure 3 and Figure S1 of the Supporting Information). Further key long-range NOEs previously described as defining the bound conformation of CsA (*50*) were also observed in the CypA−Debio 025 spectrum (Figure S1). NOE cross-peaks between MeLeu6 HN_{CH_3} and Meβmt1 HN_{CH_3}, Meβmt1 HN_{CH_3} and MeLeu10 HN_{CH_3}, and MeLeu6 HN_{CH_3} and MeLeu10 HN_{CH_3} underline the proximity of *N*-methyl protons of residues 1, 6, and 10 in Debio 025. Additional long-range NOEs equally orient the side chain of residues 1, 5, and 10 toward the center of the ring (*50*): Meβmt1 HN_{CH_3}−Val5 Hγ, MeLeu6 HN_{CH_3}−MeLeu10 Hδ, and Meβmt1 Hζ−*N*-EthVal4 Hβ. The pattern of NOE contacts shows that Debio 025 adopts the "open" conformation previously described for the CsA bound to CypA (*45*, *48*). We conclude that the overall structure of the Debio 025 peptide ring in the CypA complex is very similar to that of bound CsA. Accordingly, Debio 025 was manually constructed, starting from the CsA structure in the CypA complex (PDB entry 1CWA) and energy minimized against the CVFF force field.

The ethyl group introduced on the nitrogen at position 4 has three possible rotamers, and the same is true for the valine 4 side chain. The nine possible combinations were all generated individually and allowed to evolve in the force field. From the nine possibilities, only four different rotamer combinations were stable during the energy minimization process, with calculated energies within 5 kcal/mol of one another (Table S2 of the Supporting Information). With these conformers, we re-examined the experimental NMR spectra. The strong NOE cross-peaks connecting HN_{CH_2} of *N*-EthVal4 protons with the extremity of the lateral chain of residue Meβmt1 (Hη, Hζ, and Hε protons) and with the Hβ *N*-EthVal4 proton (Figure 3) all selected the single rotamer characterized by a value of −88° for the *N*-ethyl angle [N−Cα−C1−C2 dihedral angle (Table S2)] and 73° for the Val4 side chain χ_1 torsion angle. The Hβ protons of *N*-EthVal4 also show no NOE contact with the Hα atom of residue 5 but strong NOE contacts with the Hα atom of residue 3, again in agreement with this rotamer. Finally, in our energy-minimized structures, this rotamer was also found at the lowest total energy (Table S2). Experimental and modeling data hence all converge toward the existence of a stable conformation of Debio 025 in its complex with CypA, with a clear definition of the chemical groups that are altered in comparison with CsA. Comparison of the CsA and energy-minimized Debio 025 structures did reveal subtle effects due to the introduction of an *N*-ethyl (rather than an *N*-methyl) group at position 4. This modification indeed tends to separate

[1]Abbreviations: Meβmt1, 4(*R*)-4-[(*E*)-2-butenyl]-4-*N*-methyl-L-threonine.

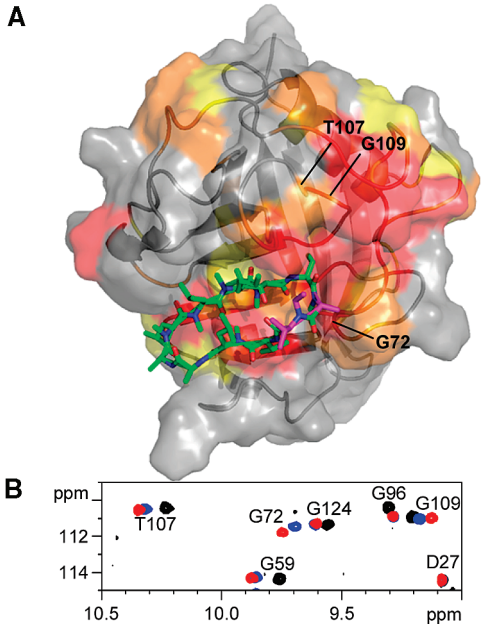

FIGURE 4: Mapping on the surface of the CypA−Debio 025 complex of the differential chemical shift observed between the CypA−CsA and CypA−Debio 025 complexes. The differences in chemical shift perturbation upon addition of CsA or Debio 025 (Figure S3 of the Supporting Information) are reported on the molecular surface of CypA (A) and colored red (combined ^{15}N and ^{1}H shift Δppm of >0.07), orange (Δppm of >0.03), or yellow (Δppm of >0.02). The side chains of residues 3 and 4 of Debio 025 are colored magenta. (B) Detailed view of superimposed HSQC spectra corresponding to CypA alone (black), the CypA−Debio 025 complex (blue), and the CypA−CsA complex (red). Annotated resonances of CypA showed the same chemical shift perturbation upon CsA or Debio 025 binding (D27, G96, and G124), or a differential perturbation depending on the ligand (G59, G72, G109, and T107).

the side chain of residue 4 farther from the D-Ala3 side chain (Figures 3 and 7). The altered spatial proximity between the *N*-ethyl Val4 protons and the MeLeu6 and Me*β*mt1 side chains is underscored by the small but significant differences in chemical shift values for those two latter residues in the CypA-bound CsA versus Debio 025 spectra (Figure 2).

Molecular NMR Structure of CypA in Its Complex with Debio 025. ^{15}N-labeled and ^{15}N- and ^{13}C-labeled CypA samples with the Debio 025 or CsA ligands were prepared, and the resulting ^{1}H−^{15}N HSQC spectra were used to map those residues that are in direct contact with the ligands. Nearly 50% of the resonances exhibited a more or less pronounced chemical shift difference upon addition of the ligand (Figure 4 and Figure S2 of the Supporting Information). Such a global perturbation of the chemical shift was already described for the interaction of the FK506 binding protein (FKBP) PPIase with the immunosuppressor ascomycin (*52*) and might be due to the fact that the ligand blocks the CypA enzyme in a particular conformation (*53*). We therefore exploited the differential chemical shift changes induced by CsA or Debio 025 binding to define the region(s) of the protein that could sense either different chemical groups or different conformations. Most of the [^{15}N]CypA resonances shifted identically upon CsA or Debio 025 binding, and only a limited number of resonances distinguish both ligands from the protein perspective (Figure 4 and Figure S2).

Together with the absence of major chemical shift differences for the common CsA and Debio 025 residues (Figure 2, Table S1 of the Supporting Information, and refs *48* and *50*), the limited differential CypA chemical shifts upon CsA or Debio 025 binding confirm the absence of major global differences in the bound conformation and position of CsA and Debio 025 in the CypA binding pocket. The CypA−CsA complex crystal structure (PDB entry 1CWA) hence is a good starting point for the construction of a CypA−Debio 025 structure, using the differential chemical shift mapping to evaluate potential differences in both complexes. The structure of the complex was obtained via replacement of the CsA ligand in the CypA−CsA complex (PDB entry 1CWA) with the minimized Debio 025 and superposition of the backbone of residues 7−10. The experimental NMR data were then used to define the parts of the molecules that were allowed to evolve during the energy minimization of the complex, residues 52−56, 63−76, and 101−112 for CypA (Figure 4 and Figure S2 of the Supporting Information) and residues 6−11 for Debio 025. Debio 025 residues 7−10 were kept fixed on the basis of the absence of chemical shift differences between both complexes (Figure 2), whereby this constraint eliminated the need to fix the translational and rotational degrees of freedom of the ligand with respect to the protein surface. With a root-mean-square deviation (rmsd) of 0.222 Å for all the Cα atoms of CypA and of 0.468 Å for the Cα atoms of those residues of CypA that were allowed to evolve during the minimization process, the resulting CypA−Debio 025 structure indicates a small conformational modification for the loops in the proximity of Debio 025 when compared to the CypA−CsA complex.

To explore further the structural basis of the differential chemical shift perturbations, we first recorded 3D NOESY-HSQC spectra on a sample of [^{15}N,^{2}H]CypA in complex with CsA or Debio 025 in aqueous buffer. Intermolecular NOEs were identified between residues Me*β*mt1, Abu2, Me-D-Ala3 (Sar3), MeLeu9, MeLeu10, and MeLeu11 of Debio 025 or CsA and CypA. In both CypA−CsA and CypA−Debio 025 complexes, identical intermolecular NOE patterns were observed for the backbone amide HN protons of Asn102, Ala103, and Gly104 and protons from the ligand (Figure 5 and Figure S3 of the Supporting Information). The HN*ε* proton in side chains of Trp121 and His126 equally displayed the same NOE patterns (Figure S3). However, comparison of NOE contacts from Gly72 HN (Figure 4) in the CypA−CsA and CypA−Debio 025 complexes showed contacts exclusively detected in the latter complex, namely toward the Me*β*mt1 HN_{CH_3} and Me-D-Ala3 HN_{CH_3} protons, despite the presence of those chemical moieties in both ligands. We can deduce from all these observations that the relative orientations of the Ala101−Phe112 loop from CypA and of the ligand are identical, while the Thr68−Gly75 loop adopts a different conformation in CypA−CsA and CypA−Debio 025 complexes. The side chain of *N*-EthVal4 sticks outward toward the solvent, and we did not observe any intermolecular NOE contacts with protein amide protons.

To pinpoint the exact nature of the chemical modification that leads to the observed differential chemical shifts in CypA−CsA and CypA−Debio 025 complexes, HSQC spectra were recorded on samples of [^{15}N]CypA and two analogues of CsA, chemically modified on the nitrogen of residue 4 with a methyl (MeVal4Cs) or an ethyl (EthVal4Cs, similar to Debio 025) but without modification of residue 3. The spectra of CypA−CsA and CypA−MeVal4Cs complexes were nearly identical, providing direct proof that the chemical modification of the side chain of residue 4 in CsA (MeLeu4 to MeVal4) does not influence the interaction. The HN_{CH_2} ethyl group at position 4 led to chemical shift modifications in the Cyp spectrum as compared to the spectrum of the

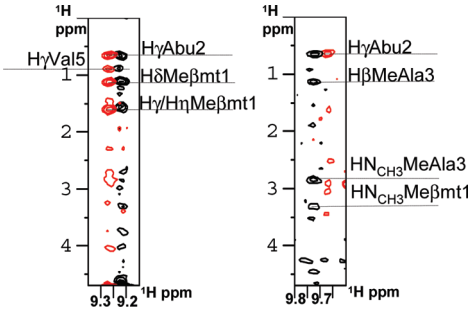

FIGURE 5: Comparison of the strips from the 3D $^{1}H-^{15}N$ NOESY spectra of [^{15}N,^{2}H]CypA in H_2O of Ala103 HN (left) and Gly72 HN (right), both residues located in loops showing differential chemical shifts in the $^{1}H-^{15}N$ HSQC spectrum upon CsA (red) or Debio 025 (black) binding (Figure 4). NOE contacts are labeled.

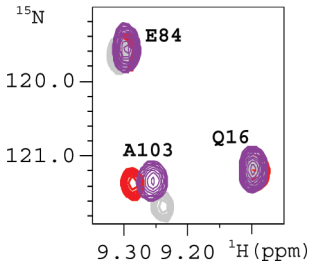

FIGURE 6: Superimposition of enlarged zones of $^{1}H-^{15}N$ HSQC spectra of [^{15}N]CypA−CsA (red), [^{15}N]CypA−Debio 025 (gray), and [^{15}N]CypA−EthVal4Cs (purple) complexes.

CypA−CsA complex but restricted to residues Asn102 and Ala103 (Figure 6). In the final structure, this loop region with differential chemical shift perturbations is in the vicinity of the additional *N*-ethyl group of *N*-EthVal4 [*d*(Ala103 Hβ−*N*-EthVal4 HN$_{CH_2}$) = 2.9 Å]. From these data, we conclude that the additional methyl group at position 3 is the sole contributor to the differential chemical shifts observed in CypA loop 63−76 and strand 52−56, and the main contributor in loop 101−112. Loop 63−76, characterized by the most important differential shifts upon CsA or Debio 025 binding [and the largest rmsd between CypA−CsA and CypA−Debio 025 complexes (rmsd = 0.511 Å)], faces directly the methyl group on residue 3 [*d*(Me-D-Ala3 Hβ−Thr73 Hα) = 2.2 Å] (Figure 3). Residue 3 in Debio 025, but not in CsA, is sufficiently close to loop 63−76 to provide NOE contacts (Figure 5) but is not at NOE distances from residues in strand 52−56 or loop 101−112. This can be explained if the shifts are not merely due to the chemical modification but also arise from a conformational modification and/or a change in dynamics due to the introduction of the methyl group at position 3 of CsA.

Homology Model of the CypA−Debio 025−CaN Complex. The absence of interaction of the cyclophilin−Debio 025 complex with CaN explains that this CsA analogue has lost its immunosuppressive character (Figure 1). To determine a structural basis for this experimental observation, we constructed a homology model of the CypA−Debio 025−CaN complex by replacing the CypA−CsA complex in the 3D structure of the CypA−CsA−CaN ternary complex [PDB entry 1M63 (*46*)] with our structure of the CypA−Debio 025 binary complex. When we focus on the interface between Debio 025 and CaN, it is clear from our model that the *N*-EthVal4 side chain of Debio 025 cannot enter the CaN hydrophobic pocket occupied by the *N*-MeLeu4 side chain of CsA in the CypA−CsA−CaN complex (Figure 7). We indeed

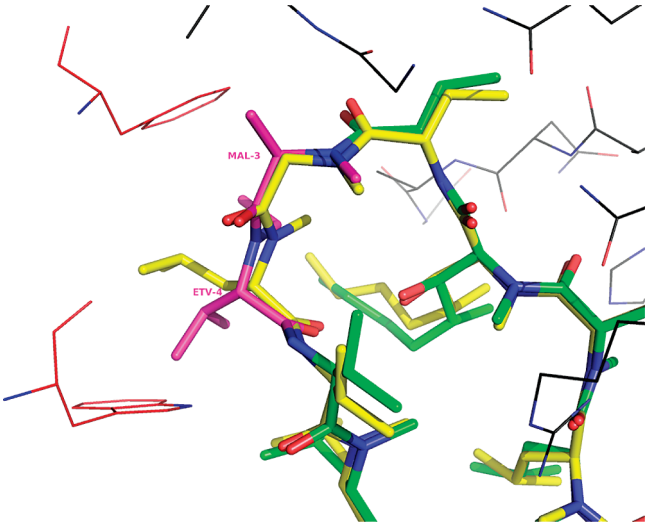

FIGURE 7: Model of the CypA−Debio 025−CaN ternary complex. CsA and Debio 025 ligands are superimposed in the binding pocket of CypA. Only the residues of CaN (red) and of CypA (black) located within 3 Å of any atom of Debio 025 (green and pink) or CsA (yellow) are represented. Nitrogen atoms are colored blue and oxygens red. The aromatic walls of the CaN hydrophobic pocket occupied in the CypA−CsA−CaN complex by the Leu4 side chain are represented as red sticks. The close contact of the *N*-EthVal4 side chain of Debio 025 with the Trp352 side chain of CaN chain A is clearly visible.

detected a clear steric clash between both methyls and the Trp352 aromatic ring that constitutes one wall of this CaN pocket. It should be pointed out that the *N*-MeLeu4 side chain adopts different orientations in the different Cyp−CsA complexes (Figure S4 of the Supporting Information), indicating a certain degree of flexibility. Comparisons of 11 CsA analog structures with the native CsA structure have accordingly shown that the largest differences are seen between the side chain conformations of residue MeLeu4 and Val5 (*54*). That flexibility seems absent in Debio 025 as the steric clash we observe in our model indeed is with the exact conformer of the Val4 side chain that we previously identified on the basis of our combined energy calculations and NOE pattern.

The *N*-ethyl group of Val4 also points toward the same CaN pocket but does not seem to cause steric hindrance in our model. However, we at present have no experimental evidence to assess the role of the *N*-ethyl moiety in the precise positioning of the Val4 side chain. Finally, the additional methyl group of residue 3 also points toward the CaN surface but does not interfere directly with the interaction.

CONCLUSIONS

We have shown that Debio 025 adopts a conformation in its complex with CypA that is very similar to that of CsA. The homology model of the CypA−Debio 025 complex with the CaN partner based on the CypA−CsA−CaN crystal structure and our CypA−Debio 025 structure indicates that the *N*-EthVal4 side chain of Debio 025 is responsible for the absence of interaction of the complex with CaN. This therefore constitutes the likely mechanism for the non-immunosuppressive character of Debio 025. The position of the lateral chain of Debio 025 residue 4, not only its chemical nature, does matter in this mechanism. The design of new candidate molecules should thus take into account the flexibility of the lateral chain of the residue pointing toward CaN to maintain the non-immunosuppressive character.

SUPPORTING INFORMATION AVAILABLE

Tables S1 and S2 and Figures S1−S4. This material is available free of charge via the Internet at http://pubs.acs.org.

REFERENCES

1. Handschumacher, R. E., Harding, M. W., Rice, J., Drugge, R. J., and Speicher, D. W. (1984) Cyclophilin: A specific cytosolic binding protein for cyclosporin A. *Science 226*, 544–547.
2. Schreiber, S. L. (1991) Chemistry and biology of the immunophilins and their immunosuppressive ligands. *Science 251*, 283–287.
3. Spik, G., Haendler, B., Delmas, O., Mariller, C., Chamoux, M., Maes, P., Tartar, A., Montreuil, J., Stedman, K., and Kocher, H. P.; et al. (1991) A novel secreted cyclophilin-like protein (SCYLP). *J. Biol. Chem. 266*, 10735–10738.
4. Price, E. R., Zydowsky, L. D., Jin, M. J., Baker, C. H., McKeon, F. D., and Walsh, C. T. (1991) Human cyclophilin B: A second cyclophilin gene encodes a peptidyl-prolyl isomerase with a signal sequence. *Proc. Natl. Acad. Sci. U.S.A. 88*, 1903–1907.
5. Fischer, G., Tradler, T., and Zarnt, T. (1998) The mode of action of peptidyl prolyl cis/trans isomerases in vivo: Binding vs. catalysis. *FEBS Lett. 426*, 17–20.
6. Liu, J., Farmer, J. D., Jr., Lane, W. S., Friedman, J., Weissman, I., and Schreiber, S. L. (1991) Calcineurin is a common target of cyclophilin-cyclosporin A and FKBP-FK506 complexes. *Cell 66*, 807–815.
7. Cardenas, M. E., Muir, R. S., Breuder, T., and Heitman, J. (1995) Targets of immunophilin-immunosuppressant complexes are distinct highly conserved regions of calcineurin A. *EMBO J. 14*, 2772–2783.
8. Luban, J., Bossolt, K. L., Franke, E. K., Kalpana, G. V., and Goff, S. P. (1993) Human immunodeficiency virus type 1 Gag protein binds to cyclophilins A and B. *Cell 73*, 1067–1078.
9. Franke, E. K., and Luban, J. (1996) Inhibition of HIV-1 replication by cyclosporine A or related compounds correlates with the ability to disrupt the Gag-cyclophilin A interaction. *Virology 222*, 279–282.
10. Braaten, D., Aberham, C., Franke, E. K., Yin, L., Phares, W., and Luban, J. (1996) Cyclosporine A-resistant human immunodeficiency virus type 1 mutants demonstrate that Gag encodes the functional target of cyclophilin A. *J. Virol. 70*, 5170–5176.
11. Chatterji, U., Bobardt, M. D., Stanfield, R., Ptak, R. G., Pallansch, L. A., Ward, P. A., Jones, M. J., Stoddart, C. A., Scalfaro, P., Dumont, J. M., Besseghir, K., Rosenwirth, B., and Gallay, P. A. (2005) Naturally occurring capsid substitutions render HIV-1 cyclophilin A independent in human cells and TRIM-cyclophilin-resistant in Owl monkey cells. *J. Biol. Chem. 280*, 40293–40300.
12. Berthoux, L., Sebastian, S., Sokolskaja, E., and Luban, J. (2005) Cyclophilin A is required for TRIM5α-mediated resistance to HIV-1 in Old World monkey cells. *Proc. Natl. Acad. Sci. U.S.A. 102*, 14849–14853.
13. Karpas, A., Lowdell, M., Jacobson, S. K., and Hill, F. (1992) Inhibition of human immunodeficiency virus and growth of infected T cells by the immunosuppressive drugs cyclosporin A and FK 506. *Proc. Natl. Acad. Sci. U.S.A. 89*, 8351–8355.
14. Lohmann, V., Korner, F., Koch, J., Herian, U., Theilmann, L., and Bartenschlager, R. (1999) Replication of subgenomic hepatitis C virus RNAs in a hepatoma cell line. *Science 285*, 110–113.
15. Nakagawa, M., Sakamoto, N., Enomoto, N., Tanabe, Y., Kanazawa, N., Koyama, T., Kurosaki, M., Maekawa, S., Yamashiro, T., Chen, C. H., Itsui, Y., Kakinuma, S., and Watanabe, M. (2004) Specific inhibition of hepatitis C virus replication by cyclosporin A. *Biochem. Biophys. Res. Commun. 313*, 42–47.
16. Watashi, K., Hijikata, M., Hosaka, M., Yamaji, M., and Shimotohno, K. (2003) Cyclosporin A suppresses replication of hepatitis C virus genome in cultured hepatocytes. *Hepatology 38*, 1282–1288.
17. Nakagawa, M., Sakamoto, N., Tanabe, Y., Koyama, T., Itsui, Y., Takeda, Y., Chen, C. H., Kakinuma, S., Oooka, S., Maekawa, S., Enomoto, N., and Watanabe, M. (2005) Suppression of hepatitis C virus replication by cyclosporin a is mediated by blockade of cyclophilins. *Gastroenterology 129*, 1031–1041.
18. Ryffel, B., Woerly, G., Murray, M., Eugster, H. P., and Car, B. (1993) Binding of active cyclosporins to cyclophilin A and B, complex formation with calcineurin A. *Biochem. Biophys. Res. Commun. 194*, 1074–1083.
19. Watashi, K., Ishii, N., Hijikata, M., Inoue, D., Murata, T., Miyanari, Y., and Shimotohno, K. (2005) Cyclophilin B is a functional regulator of hepatitis C virus RNA polymerase. *Mol. Cell 19*, 111–122.
20. Yang, F., Robotham, J. M., Nelson, H. B., Irsigler, A., Kenworthy, R., and Tang, H. (2008) Cyclophilin A is an essential cofactor for hepatitis C virus infection and the principal mediator of cyclosporine resistance in vitro. *J. Virol. 82*, 5269–5278.
21. Kaul, A., Stauffer, S., Berger, C., Pertel, T., Schmitt, J., Kallis, S., Lopez, M. Z., Lohmann, V., Luban, J., and Bartenschlager, R. (2009) Essential role of cyclophilin A for hepatitis C virus replication and virus production and possible link to polyprotein cleavage kinetics. *PLoS Pathog. 5*, e1000546.
22. Liu, Z., Yang, F., Robotham, J. M., and Tang, H. (2009) Critical role of cyclophilin A and its prolyl-peptidyl isomerase activity in the structure and function of the hepatitis C virus replication complex. *J. Virol. 83*, 6554–6565.
23. Chatterji, U., Bobardt, M., Selvarajah, S., Yang, F., Tang, H., Sakamoto, N., Vuagniaux, G., Parkinson, T., and Gallay, P. (2009) The isomerase active site of cyclophilin a is critical for hepatitis C virus replication. *J. Biol. Chem. 284*, 16998–17005.
24. Goto, K., Watashi, K., Inoue, D., Hijikata, M., and Shimotohno, K. (2009) Identification of cellular and viral factors related to anti-hepatitis C virus activity of cyclophilin inhibitor. *Cancer Sci. 100*, 1943–1950.
25. Gaither, L. A., Borawski, J., Anderson, L. J., Balabanis, K. A., Devay, P., Joberty, G., Rau, C., Schirle, M., Bouwmeester, T., Mickanin, C., Zhao, S., Vickers, C., Lee, L., Deng, G., Baryza, J., Fujimoto, R. A., Lin, K., Compton, T., and Wiedmann, B. (2009) Multiple cyclophilins involved in different cellular pathways mediate HCV replication. *Virology 397*, 43–55.
26. Heck, J. A., Meng, X., and Frick, D. N. (2009) Cyclophilin B stimulates RNA synthesis by the HCV RNA dependent RNA polymerase. *Biochem. Pharmacol. 77*, 1173–1180.
27. Fernandes, F., Poole, D. S., Hoover, S., Middleton, R., Andrei, A. C., Gerstner, J., and Striker, R. (2007) Sensitivity of hepatitis C virus to cyclosporine A depends on nonstructural proteins NS5A and NS5B. *Hepatology 46*, 1026–1033.
28. Waller, H., Chatterji, U., Gallay, P., Parkinson, T., and Targett-Adams, P. (2010) The use of AlphaLISA technology to detect interaction between hepatitis C virus-encoded NS5A and cyclophilin A. *J. Virol. Methods 165*, 202–210.
29. Puyang, X., Poulin, D. L., Mathy, J. E., Anderson, L. J., Ma, S., Fang, Z., Zhu, S., Lin, K., Fujimoto, R., Compton, T., and Wiedmann, B. (2010) Mechanism of Resistance of HCV Replicons to Structurally Distinct Cyclophilin Inhibitors. *Antimicrob. Agents Chemother*. DOI 10.1128/AAC.01236-09.
30. Ciesek, S., Steinmann, E., Wedemeyer, H., Manns, M. P., Neyts, J., Tautz, N., Madan, V., Bartenschlager, R., von Hahn, T., and Pietschmann, T. (2009) Cyclosporine A inhibits hepatitis C virus nonstructural protein 2 through cyclophilin A. *Hepatology 50*, 1638–1645.
31. Jaeckel, E., Cornberg, M., Wedemeyer, H., Santantonio, T., Mayer, J., Zankel, M., Pastore, G., Dietrich, M., Trautwein, C., and Manns, M. P. (2001) Treatment of acute hepatitis C with interferon α-2b. *N. Engl. J. Med. 345*, 1452–1457.
32. Craxi, A., and Licata, A. (2003) Clinical trial results of peginterferons in combination with ribavirin. *Semin. Liver Dis. 23* (Suppl. 1), 35–46.
33. Watashi, K., and Shimotohno, K. (2007) Cyclophilin and viruses: Cyclophilin as a cofactor for viral Infection and possible Anti-Viral Target. *Drug Target Insights 1*, 9–18.
34. Watashi, K., and Shimotohno, K. (2007) Chemical genetics approach to hepatitis C virus replication: Cyclophilin as a target for anti-hepatitis C virus strategy. *Rev. Med. Virol. 17*, 245–252.
35. Goto, K., Watashi, K., Murata, T., Hishiki, T., Hijikata, M., and Shimotohno, K. (2006) Evaluation of the anti-hepatitis C virus effects of cyclophilin inhibitors, cyclosporin A, and NIM811. *Biochem. Biophys. Res. Commun. 343*, 879–884.
36. Neyts, J. (2006) Selective inhibitors of hepatitis C virus replication. *Antiviral Res. 71*, 363–371.
37. Hubler, F., Rückle, T., Patiny, L., Muamba, T., Guichou, J.-F., Mutter, M., and Wenger, R. (2000) Synthetic routes to NEtXaa^4-cyclosporine A derivatives as potential anti-HIV I drugs. *Tetrahedron Lett. 41*, 7193–7196.
38. Paeshuyse, J., Kaul, A., De Clercq, E., Rosenwirth, B., Dumont, J. M., Scalfaro, P., Bartenschlager, R., and Neyts, J. (2006) The non-immunosuppressive cyclosporin DEBIO-025 is a potent inhibitor of hepatitis C virus replication in vitro. *Hepatology 43*, 761–770.
39. Coelmont, L., Kaptein, S., Paeshuyse, J., Vliegen, I., Dumont, J. M., Vuagniaux, G., and Neyts, J. (2009) Debio 025, a cyclophilin binding molecule, is highly efficient in clearing hepatitis C virus (HCV) replicon-containing cells when used alone or in combination with specifically targeted antiviral therapy for HCV (STAT-C) inhibitors. *Antimicrob. Agents Chemother. 53*, 967–976.
40. Inoue, K., Umehara, T., Ruegg, U. T., Yasui, F., Watanabe, T., Yasuda, H., Dumont, J. M., Scalfaro, P., Yoshiba, M., and Kohara, M. (2007)

Evaluation of a cyclophilin inhibitor in hepatitis C virus-infected chimeric mice in vivo. *Hepatology 45*, 921–928.
41. Flisiak, R., Horban, A., Gallay, P., Bobardt, M., Selvarajah, S., Wiercinska-Drapalo, A., Siwak, E., Cielniak, I., Higersberger, J., Kierkus, J., Aeschlimann, C., Grosgurin, P., Nicolas-Metral, V., Dumont, J. M., Porchet, H., Crabbe, R., and Scalfaro, P. (2008) The cyclophilin inhibitor Debio-025 shows potent anti-hepatitis C effect in patients coinfected with hepatitis C and human immunodeficiency virus. *Hepatology 47*, 817–826.
42. Flisiak, R., Feinman, S. V., Jablkowski, M., Horban, A., Kryczka, W., Pawlowska, M., Heathcote, J. E., Mazzella, G., Vandelli, C., Nicolas-Metral, V., Grosgurin, P., Liz, J. S., Scalfaro, P., Porchet, H., and Crabbe, R. (2009) The cyclophilin inhibitor Debio 025 combined with PEG IFNα2a significantly reduces viral load in treatment-naive hepatitis C patients. *Hepatology 49*, 1460–1468.
43. Ptak, R. G., Gallay, P. A., Jochmans, D., Halestrap, A. P., Ruegg, U. T., Pallansch, L. A., Bobardt, M. D., de Bethune, M. P., Neyts, J., De Clercq, E., Dumont, J. M., Scalfaro, P., Besseghir, K., Wenger, R. M., and Rosenwirth, B. (2008) Inhibition of human immunodeficiency virus type 1 replication in human cells by Debio-025, a novel cyclophilin binding agent. *Antimicrob. Agents Chemother. 52*, 1302–1317.
44. Tiepolo, T., Angelin, A., Palma, E., Sabatelli, P., Merlini, L., Nicolosi, L., Finetti, F., Braghetta, P., Vuagniaux, G., Dumont, J. M., Baldari, C. T., Bonaldo, P., and Bernardi, P. (2009) The cyclophilin inhibitor Debio 025 normalizes mitochondrial function, muscle apoptosis and ultrastructural defects in Col6a1(−/−) myopathic mice. *Br. J. Pharmacol. 157*, 1045–1052.
45. Mikol, V., Kallen, J., Pflugl, G., and Walkinshaw, M. D. (1993) X-ray structure of a monomeric cyclophilin A-cyclosporin A crystal complex at 2.1 Å resolution. *J. Mol. Biol. 234*, 1119–1130.
46. Huai, Q., Kim, H. Y., Liu, Y., Zhao, Y., Mondragon, A., Liu, J. O., and Ke, H. (2002) Crystal structure of calcineurin-cyclophilin-cyclosporin shows common but distinct recognition of immunophilin-drug complexes. *Proc. Natl. Acad. Sci. U.S.A. 99*, 12037–12042.
47. Ottiger, M., Zerbe, O., Guntert, P., and Wuthrich, K. (1997) The NMR solution conformation of unligated human cyclophilin A. *J. Mol. Biol. 272*, 64–81.
48. Weber, C., Wider, G., von Freyberg, B., Traber, R., Braun, W., Widmer, H., and Wuthrich, K. (1991) The NMR structure of cyclosporin A bound to cyclophilin in aqueous solution. *Biochemistry 30*, 6563–6574.
49. Neri, P., Gemmecker, G., Zydowsky, L. D., Walsh, C. T., and Fesik, S. W. (1991) NMR studies of [U-^{13}C]cyclosporin A bound to human cyclophilin B. *FEBS Lett. 290*, 195–199.
50. Fesik, S. W., Gampe, R. T., Jr., Eaton, H. L., Gemmecker, G., Olejniczak, E. T., Neri, P., Holzman, T. F., Egan, D. A., Edalji, R., and Simmer, R.; et al. (1991) NMR studies of [U-^{13}C]cyclosporin A bound to cyclophilin: Bound conformation and portions of cyclosporin involved in binding. *Biochemistry 30*, 6574–6583.
51. Hsu, V. L., and Armitage, I. M. (1992) Solution structure of cyclosporin A and a non-immunosuppressive analog bound to fully deuterated cyclophilin. *Biochemistry 31*, 12778–12784.
52. Medek, A., Hajduk, P. J., Mack, J., and Fesik, S. W. (2000) The Use of Differential Chemical Shifts for Determining the Binding Site Location and Orientation of Protein-Bound Ligands. *J. Am. Chem. Soc. 122*, 1241–1242.
53. Fraser, J. S., Clarkson, M. W., Degnan, S. C., Erion, R., Kern, D., and Alber, T. (2009) Hidden alternative structures of proline isomerase essential for catalysis. *Nature 462*, 669–673.
54. Kallen, J., Mikol, V., Taylor, P., and Walkinshaw, M. D. (1998) X-ray structures and analysis of 11 cyclosporin derivatives complexed with cyclophilin A. *J. Mol. Biol. 283*, 435–449.